*International Journal Of Engineering Research And Development*
*e- ISSN: 2278-067X, p-ISSN: 2278-800X, www.ijerd.com*
*Volume 21, Issue 1 (January, 2025), PP 218-226*

# Adaptive-COA-ELM based-Fault Diagnosis Method for Electric Vehicle Charging Equipment

Sheng Dou[1,2*], Wentao Lu[1,2], Chang Liu[3]
[1] *State Grid Electric Power Research Institute, Nanjing 210000, China*
[2] *NARI Technology Co. Ltd., Nanjing 210000, China*
[3] *State Grid Shanghai Electric Power Co. Ltd., Shanghai 200000, China*
**Corresponding Author: Sheng Dou.*

***ABSTRACT:*** *Considering electric vehicle charging equipment breaks down frequently, a fault diagnosis method based on an improved Extreme Learning Machine (ELM) is proposed to address frequent and difficult-to-accurately-diagnose faults in electric vehicle charging equipment. Firstly, Random Forest is utilized to extract fault characteristic parameters of the charging equipment as the dataset for model training. Secondly, an improved Crayfish Optimization Algorithm (COA) is introduced to optimize the output weights in the ELM model, resulting in an optimized model. Lastly, the optimization model is employed to diagnose faults in electric vehicle charging equipment. Simulation results demonstrate that this method achieves higher accuracy compared to other technologies, thereby validating the reliability of the fault diagnosis approach based on adaptive-COA-ELM. This holds significant importance for the research and application of electric vehicle charging equipment fault diagnosis.*

***Keywords:*** *EV charging equipment; fault diagnosis; Crayfish Optimization Algorithm; Extreme Learning Machine*

---

Date of Submission: 11-01-2025 Date of acceptance: 23-01-2025

---

## I. INTRODUCTION

Given the tight energy supply situation, the electric vehicle industry is thriving. Unlike the traditional fuel vehicle industry, the field of electric vehicles represents a nascent and rapidly evolving sector, and its related technologies are still in a process of continuous exploration and optimization[[1]]. Especially the charging equipment of electric vehicles plays a crucial role in the operational performance of the vehicle. Therefore, fault diagnosis and analysis of electric vehicle charging equipment are particularly important.

Scholars both domestically and internationally have proposed corresponding research methods for diagnosing faults in charging equipment. Hou Junjie[[2]] focuses on improving the safety and stability of charging equipment, accelerating the fault handling process, and envisioning and implementing a system based on B/S architecture and ASP NET technology for monitoring the status and remote fault diagnosis of electric vehicle charging facilities. Gao Hui et al[[3]] explored the safety integration mechanism between power battery, charging pile, and power supply equipment, a set of integrated fault logic judgment processes was designed, and a fault tree model of phased online fault diagnosis of equipment was constructed. The variety of fault types in charging equipment poses a serious challenge to traditional diagnostic methods. These methods often rely on human experience and preset rules, making it difficult to identify and deal with new or complex faults quickly and effectively. To cope with this problem, scholars have turned their attention to artificial intelligence technology. Park, S. J. et al[[4]]create a data collection system to assess module statuses by utilizing the gathered information and implementing a Multi-Layer Perceptron (MLP) neural network for classification model training. Meanwhile, Meckel S. et al[[5]] introduce a structured machine-learning approach to develop an online diagnostic system for hybrid electric vehicle models. Mao Min et al[[6]] propose an improved backpropagation neural network, the simulation demonstrates that the optimized BP model provides both rapid and accurate fault state diagnosis for the charging pile. The intelligent algorithms mentioned by these scholars have improved the fault diagnosis rate of charging equipment to a certain extent. However, there are still certain deficiencies in accuracy and diagnosis speed[[7]].

Based on the above analysis, because of the challenges faced in the current fault diagnosis of charging equipment, an improved COA is proposed. This algorithm focuses on enhancing the parameter configuration and structural design of the ELM to improve its effectiveness as a fault diagnosis model. Specifically, by introducing the dominant characteristics of crayfish in nature, we designed a more efficient search mechanism to

improve the accuracy and robustness of ELM in fault diagnosis tasks. Comparative experiments will validate the enhanced algorithm's superior capabilities in recognizing complex fault modes, which not only provides a new idea for the fault diagnosis of charging equipment but also opens up a new direction for the application of intelligent algorithms in related fields.

## II. CHARGING INDICATORS FOR ELECTRIC VEHICLE CHARGING EQUIOMENT

### 2.1.Charging equipment analysis

EV charging equipment is an important part of EV infrastructure, and its core function is to provide a safe and efficient power supply for EVs. The charging equipment is mainly composed of two parts: the charger and the charging pile[[8]]. The charger is the core component of the whole system, which is mainly responsible for converting the alternating current (AC) energy of the grid into direct current (DC) suitable for EV battery charging and adjusting the output power to ensure a stable charging voltage and current for the EV. Chargers typically use advanced power electronics, such as insulated-gate bipolar transistors (IGBT modules), to achieve efficient and precise power conversion and power control[[9]]. The charging structure of an electric vehicle is shown in Figure 1.

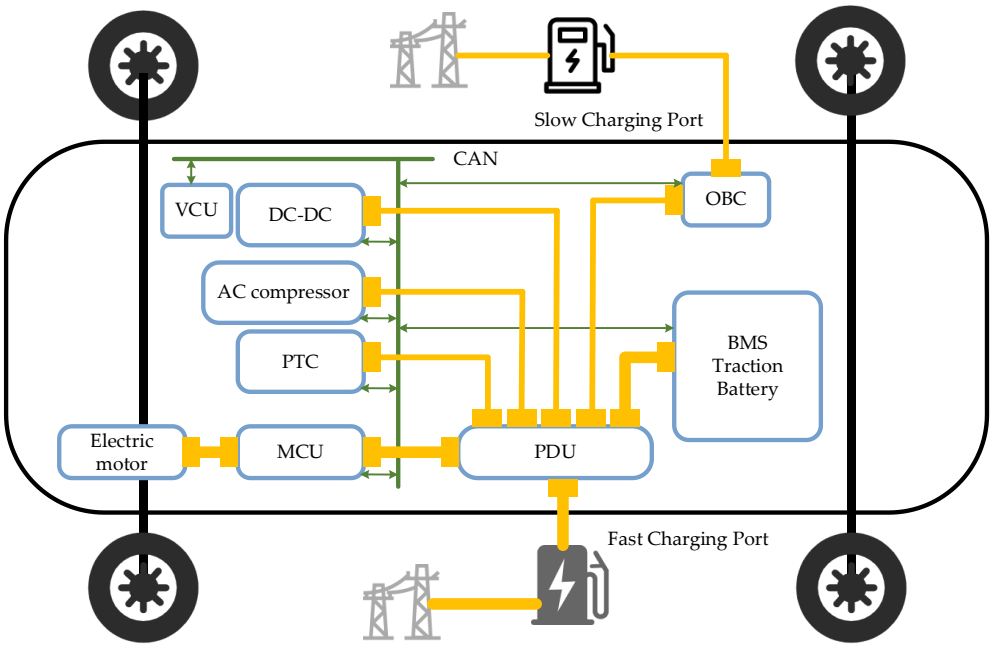


**Figure 1. Charging structure of an electric vehicle**

### 2.2. Charging equipment fault type analysis

Due to the complex physical hardware structure of the charging equipment and the changeable working state, there are many kinds of failures. This paper combs and summarizes the fault data of charging equipment collected in the actual operation process. This data covers different brands, models, and operating environments, providing a valuable basis for analyzing failure modes. Through in-depth mining of these data, we summarize and analyze the common fault types of charging equipment and their corresponding fault causes, and the specific summary results are detailed in Table 1.

**Table 1. The common faults and causes of faults of charging equipment**

| Fault number | Description of the fault | Cause of the failure |
|---|---|---|
| 1 | Normal state | - |
| 2 | The charging module outputs an overvoltage | The output voltage of a single module is too large, causing the system to have overcurrent protection |
| 3 | The charging module outputs an overcurrent | The output current of the charging module exceeds the preset value of the system |
| 4 | The charging module is over-temperature faulty | (1) The charging module fan is faulty<br>(2) The temperature setpoint is on the low side<br>(3) The temperature sensor is faulty |
| 5 | The DC bus outputs an overvoltage | (1) The impulse voltage on the output side of the DC bus is too large, and the output of the module is out of control |
| 6 | Faulty AC circuit breaker | (1) The circuit breaker tripped |

| | | |
|---|---|---|
| | | (2) The circuit breaker device is damaged<br>(3) Short circuit or overcurrent |
| 7 | BMS communication failure | (1) BMS system failure<br>(2) The vehicle does not receive auxiliary power<br>(3) Poor contact with the charging connector |
| 8 | AC input failure | (1) AC power failure<br>(2) AC input is out of phase<br>(3) AC input overvoltage |

### 2.3. Random forest-based fault feature parameter extraction of charging equipment

During the operation of EV charging equipment, the information transmitted is key to ensuring effective, safe, and efficient charging, and this information covers several important parameters. Based on the research results, there is a strong coupling relationship and nonlinear characteristics between the fault characteristic parameters of electric vehicle charging equipment. With the help of the multivariate spatiotemporal relationship analysis method, the intrinsic relationship between the state data of charging equipment can be explored. This paper employs the random forest algorithm[[10],[11]] to assess the importance of the aforementioned monitoring parameters in determining the fault diagnosis outcomes of charging equipment. As a robust ensemble learning approach, the random forest method effectively evaluates the impact of each input feature on the final result. It achieves this by constructing a large number of decision trees, combining their prediction results through voting, and ultimately deriving the final diagnosis outcome. During the training phase, the algorithm systematically evaluates the significance of each feature during node splitting to rank their contributions. Leveraging the random forest algorithm's ranking results, we identified the key data with the greatest influence on fault diagnosis outcomes and utilized these as input for subsequent model training. The fault characteristic parameters are summarized in Table 2.

**Table 2. Fault characteristic parameters of charging equipment**

| Serial number | Description | Label |
|---|---|---|
| 1 | Charging device voltage | #1 |
| 2 | Charging device current | #2 |
| 3 | Electric vehicles demand voltage | #3 |
| 4 | Electric vehicles demand current | #4 |
| 5 | DC bus voltage | #5 |
| 6 | Charging device temperature | #6 |
| 7 | EV charging time | #7 |
| 8 | Charging equipment fault, power supply voltage | #8 |

## III. FAULT DIAGNOSIS METHOD BASED ON ADPTIVE-COA-ELM

### 3.1. Extreme learning machine model

ELM [[12],[13]]is a computationally efficient single-hidden layer feedforward neural network, that has gained significant traction in machine learning and pattern recognition. Figure 2 provides a visual representation of the ELM's structure and the interconnection of its layers.

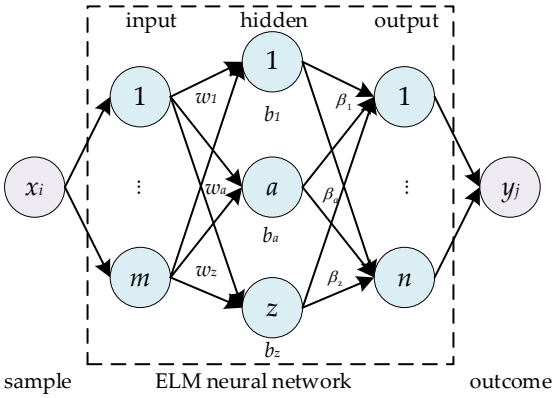


**Figure 2. ELM model structural diagram**

ELM distinguishes itself from traditional feedforward networks through its unique architecture and training approach, leading to enhanced computational speed and generalization capability, particularly when tackling complex problems. The ELM model comprises an input, a hidden, and an output layer, interconnected

via feature mappings that establish a complete pathway for information flow and processing. According to the structure diagram, the ELM algorithm is shown below，

$$y_j = \sum_{i=1}^{N} \beta_i g(x_i) = \sum_{i=1}^{m} \beta_i g\left(w_i \cdot x_i + b_i\right) \qquad j = 1, 2, \cdots, n \tag{1}$$

$$x_i = (x_{i1}, x_{i2}, \cdots x_{im})^T \in R^m \tag{2}$$

$$y_i = (y_{j1}, y_{j2}, \cdots y_{jn})^T \in R^n \tag{3}$$

$w_i = \left(w_{i1}, w_{i2}, \cdots w_{im}\right)^T$ is the weight of the input layer to the hidden layer, $\beta_i = (\beta_{i1}, \beta_{i2}, \cdots \beta_{in})^T$ is the weight from the hidden layer to the output layer, $g(\cdot)$ is the hidden layer activation function, and $b_i$ is the hidden layer deviation, the output of the ELM is

$$Y = H\beta \tag{4}$$

$$H(w_1, \cdots, w_z, b_1, \cdots, b_z, x_1, \cdots, x_m) = \begin{bmatrix} g(w_1 \cdot x_1 + b_1) & \cdots & g(w_m \cdot x_1 + b_z) \\ \vdots & \ddots & \vdots \\ g(w_1 \cdot x_m + b_1) & \cdots & g(w_m \cdot x_m + b_1) \end{bmatrix} \tag{5}$$

The output weight matrix is obtained by solving the linear system

$$\tilde{\beta} = H^{+}Y \tag{6}$$

$H^+$ is the generalized inverse matrix of $H$.

### 3.2. Adaptive Crayfish Optimization Algorithm

The COA is a novel swarm intelligence optimization algorithm proposed by Professor Heming Jia in 2023[[14]]. The algorithm's design is influenced by the behavioral patterns of crayfish in their natural habitat, particularly focusing on three main behaviors: foraging, heat avoidance, and competition. As a highly adaptable organism, crayfish can survive in complex aquatic environments, and its behavioral characteristics provide unique inspiration for the design of optimization algorithms.

In COA, the act of escaping the heat (Evasion) is seen as central to the exploration phase. Crayfish actively seek out cool habitats in hot environments to avoid the threat of extreme temperatures to their survival. In the algorithm, this behavior is modeled as a global search mechanism, where random walks or perturbation techniques are employed to explore various regions of the solution space, thereby preventing convergence to local optima. The introduction of summer avoidance behavior makes COA have a strong global exploration ability and can effectively discover potential excellent solutions.

Foraging behavior reflects the strategy of crayfish in search of food resources, manifested by meticulous search of their surroundings and pursuit of food. This behavior is implemented as a local search process in the algorithm, refining the solution within the vicinity of the current solution to enhance its quality. Competitive behavior, on the other hand, simulates the adversarial interaction of crayfish in competition for limited resources. Competitive behavior is reflected in the interactions among individuals, fostering continuous improvement of the solution through a competitive mechanism.

In general, COA cleverly combines global exploration with local development by simulating the foraging, heat avoidance, and competitive behavior of crayfish, forming an optimization algorithm with both diversity and efficiency[[15]].

#### 3.2.1 Crayfish Optimization Algorithm

(1) Summer retreat stage

The crayfish optimization algorithm employs a mathematical model to represent crayfish feed intake $p$, factoring in the impact of ambient temperature. This relationship is defined by equation (7).

$$temp = r \cdot 15 + 20 \tag{7}$$

$$p = C_1 \cdot \left(\frac{1}{\sqrt{2\pi} \cdot \sigma} \exp\left(-\frac{(temp - \mu)^2}{2\sigma^2}\right)\right) \tag{8}$$

The range of *temp* is set from 20℃ to 35℃, and 25℃ is determined to be the most ideal foraging temperature, $r$ is a random number ranging from 0 to 1, $\mu$ represents the optimal temperature for crayfish to feed, $C_1$ is a constant 0.2, and $\sigma$ is a constant 3, which can be adjusted to control the amount of crayfish at different temperatures[[16]].

When *temp*>30℃, the crayfish will enter the summer retreat stage, and the summer shelter position $X_s$ is shown in equation (9).

$$X_s = (X_G + X_L)/2 \tag{9}$$

$X_G$ denotes the global best position and $X_L$ represents the current population's local best. In the summer burrow competition phase, where $r < 0.5$, the location is updated using the formula (10).

$$X_{i,j}^{t+1} = X_{i,j}^{t} + C_2 \cdot r \cdot (X_s - X_{i,j}^{t}) \tag{10}$$

$t$ indicates the current iteration count, while $X_{i,j}^{t}$ represents the j-dimensional position of the ith crayfish during the tth iteration is represented. Additionally, $C_2$ signifies a descending curve that ranges from 2 to 0, as illustrated in equation (11).

$$C_2 = 2 - (temp / T) \tag{11}$$

where $T$ is the maximum number of iterations.

(2) Competitive stage

When $temp$>30℃ and $r \geq 0.5$, it indicates that there are other crayfish participating in the competition, and the position update formula of crayfish is shown in (12).

$$X_{i,j}^{t+1} = X_{i,j}^{t} - X_{z,j}^{t} + X_s \tag{12}$$

$z$ represents another randomly obtained crayfish individual, and the formula is as follows,

$$z = round(r \cdot (\text{N-1})) + 1 \tag{13}$$

N is the number of crayfish populations.

(3) Foraging stage

When $temp \leq 30$℃, crayfish will locate food, they assess its size. If the food is too large, they will break it into smaller pieces before consuming it; if the size is appropriate, they will eat it directly. The position of the food is denoted as $X_f$, where $X_f = X_G$,, and the size of the food $Q$ is defined as detailed in equation (14).

$$Q = C_3 \cdot r \cdot (fitness_i / fitness_{food}) \tag{14}$$

$C_3$ is a constant food factor set to 3. $fitness_i$ represents the fitness of the ith crayfish, and $fitness_{food}$ is the fitness of the food source. When $Q > (C_3 + 1)/2$, signifying overly large food, the crayfish's decomposition process is modeled using a combination of sine and cosine functions, detailed in equations (15) and (16).

$$X_f = \exp(-\frac{1}{Q}) \cdot X_f \tag{15}$$

$$X_{i,j}^{t+1} = X_{i,j}^{t} + X_f \cdot p \cdot (\cos(2\pi r) - \sin(2\pi r)) \tag{16}$$

When $Q \leq (C_3 + 1)/2$, The crayfish simply moves towards the food position and eats, the formula is:

$$X_{i,j}^{t+1} = (X_{i,j}^{t} - X_f) \cdot p + p \cdot r \cdot X_{i,j}^{t} \tag{17}$$

3.2.2 Adaptive Crayfish Optimization Algorithm

While the Crayfish Optimization Algorithm (COA) is a promising new swarm intelligence optimization method with numerous advantages, it also has certain limitations that merit consideration. The advantage of COA lies in its powerful global search ability, which is due to its simulation of crayfish's summer escape behavior, which enables the algorithm to carry out extensive exploration in the solution space and avoid falling into the local optimal prematurely. However, the performance of COAs is also limited by several factors. Firstly, the effectiveness of the COA is significantly influenced by the initial population distribution. A poor initial distribution can hinder the algorithm's search efficiency and convergence rate. Secondly, the COA tends to exhibit relatively slow local convergence. Due to its main focus on global exploration, its ability in local search is relatively weak, so it may not be able to quickly converge to the optimal solution in the later stage of search. In addition, the search efficiency of COA is not stable, and its performance may fluctuate greatly under different optimization problems and parameter settings, which makes it necessary to carry out a lot of parameter adjustment and experimental verification in practical applications. More critically, COAs tend to fall into local optimals. Therefore, in this paper, ACOA was established around the initial population distribution and attenuation factor of crayfish, and the specific improvements are as follows[[17]].

(1) Chaos is initially dissolved

The initial solution is set by random initialization in COA, which may lead to uneven distribution of individual positions and lack of flexibility. To overcome this problem, Circle mapping is introduced as an alternative. Specifically, by introducing chaos mapping, the algorithm can cover a wider solution space at the initial stage, ensuring that the potential global optimal solution can be more fully explored. The introduction of this method directly improves the global search capability of COA, enabling it to find the global optimal solution more efficiently when facing complex optimization problems. The expression for Circle mapping is as follows,

$$X_{i+1} = \mathrm{mod}(X_i + l - \frac{k}{2\pi}\sin(2\pi X_i), 1) \quad (18)$$

where $i$ represents the number of iterations, $l$=0.5, $k$=0.2; $X_i$ is the individual position of the population after chaos mapping, and mod represents the remainder operation.

(2) Nonlinear convergence factor

The attenuation factor $C_2$ in the COA is a static constant, which restricts the algorithm's global exploration and exploitation capabilities. To address this, an improved nonlinear convergence factor is employed in place of $C_2$ to enhance the algorithm's convergence rate, as described in equation (19).

$$\alpha(t) = \frac{\alpha_1 - \alpha_0}{\lg(\alpha_1 - \alpha_0)} \lg(\alpha_1 - \alpha_0 - (\frac{t}{T+1})) \quad (19)$$

where $\alpha_1$ means that the initial value of the control factor is 2, and $\alpha_0$ means that the final value of the control silver is 0, replace $C_2$ with equation (10) to complete the update of the formula.

### 3.3. Adaptive-COA-ELM

Introducing the ACOA algorithm to optimize the output weights of the ELM allows for a more effective exploration of the solution space and facilitates the identification of optimal output weight solutions. Flow chart of the ELM model optimized by the ACOA as Figure 4. The specific steps are as follows.

**Step 1:** Initialize algorithm parameters.

**Step 2:** Determine the network fitness function, calculate the fitness value, and determine the initial optimal solution.

**Step 3:** If the temperature temp>30, define the elite cave according to equation (9).

**Step 4:** If the random number r<0.5, according to equation (10), the crayfish enters the summer stage, otherwise, according to equation (11), the crayfish enters the competitive stage.

**Step 5:** If the temperature temp<30, define the foraging volume p and size of the food Q according to equations (8) and (14).

**Step 6:** If the size of the food Q>($C_3$+1)/2, eating is simulated according to equations (15) and (16), otherwise, eating is simulated according to equations (17).

**Step 7:** Update the optimal solution

**Step 8:** If the number of iterations is reached, obtain the global optimal solution and calculate the optimal output weight of the ELM; otherwise, return to step 3.

**Step 9:** Calculate the error, and update the output weights.

**Step 10:** If the number of iterations is reached, output the optimal solution and optimal value; otherwise, return to step 9.

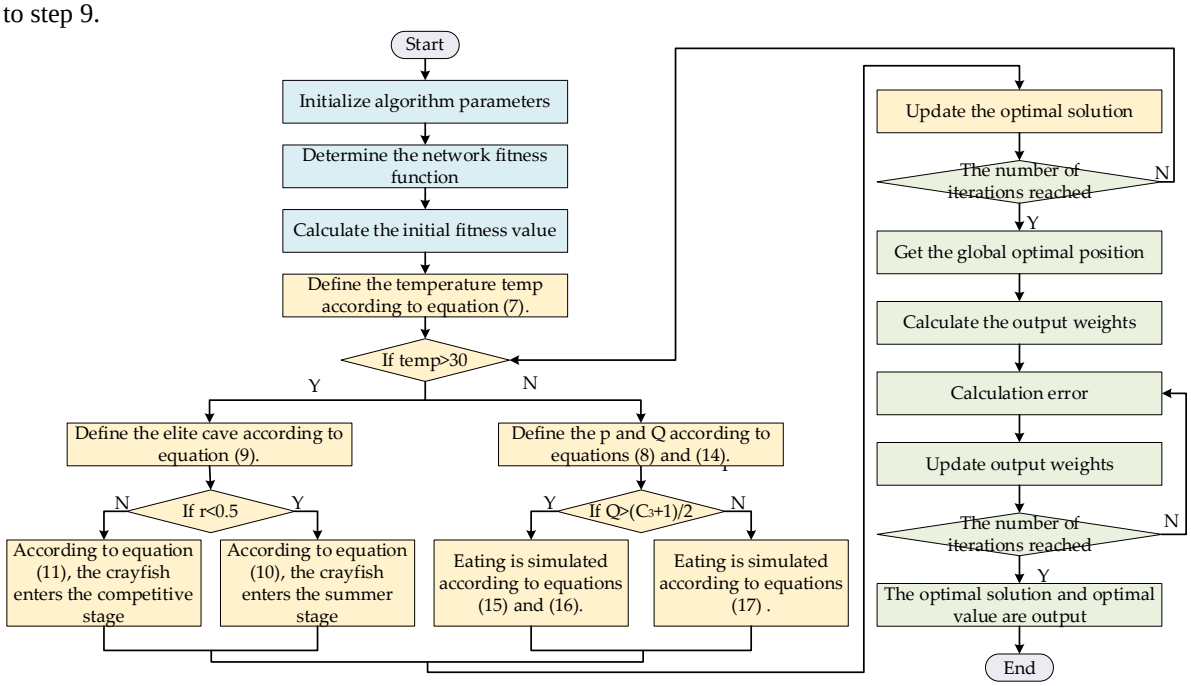


**Figure 3. ACOA-ELM flow chart**

## IV. EXPERIMENT AND DISCUSSION

### 4.1. Data preprocessing

In this part, EV charging equipment fault data in a certain area in 2024 are randomly selected as data inputs, and fault diagnosis accuracy as output. Data preprocessing can provide a high-quality foundation for subsequent model training and analysis. After the data is preprocessed accordingly, there are a total of 120 sets of experimental test sample data. Among them, 60 sets of EV charging equipment fault data are used to train a fault diagnosis model to ensure that the model can fully capture the characteristics and patterns of EV charging equipment faults. The performance of the fault diagnosis model was tested using 60 sets of EV charging equipment fault data, which can more realistically reflect the performance of the model in real-world applications.

### 4.2. Case analysis

In the fault diagnosis model constructed in this paper, precise parameters should be set to ensure the best prediction performance and computational efficiency. The number of neurons in the input layer is set to 10. In the hidden layer of the model, the number of neurons is a crucial parameter, after considering the balance between improving prediction accuracy and maintaining computational efficiency, we set the number of neurons in the hidden layer to 50. In addition, the number of neurons in the output layer is set to 1, mainly because the fault diagnosis output is single, which can characterize the fault state of the device. In the overall structure design of the whole network, the population size of the model is also set to 20, to control the complexity of the model, and ensure that it can work efficiently with reasonable computing resources. Finally, we set the maximum number of iterations to 50.

Compare the optimized model in this article with ELM, PSO-ELM[[18]], and COA-ELM, the fitness value is crucial for evaluating the convergence and optimization performance of algorithms, Figure 7 presents the population fitness variation curves of PSO, COA, and ACOA optimization processes. In the figure, it can be seen that ACOA achieves the lowest fitness value within the number of iterations, indicating that the optimization effect is the best.

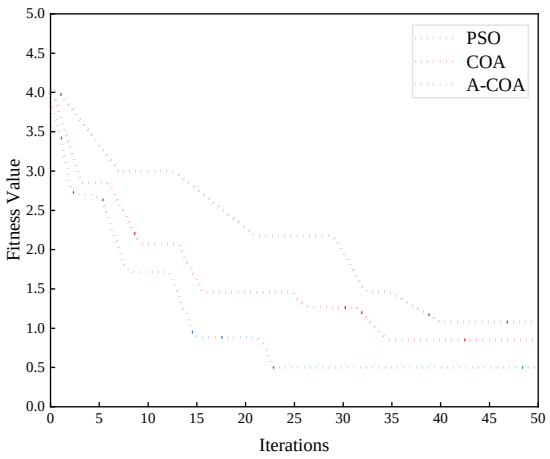


**Figure 4. Optimization algorithm fitness curve of different models**

To assess the effectiveness of our proposed improvement, we conducted several comparative experiments. The results indicate that our method significantly outperforms the traditional ELM model in diagnosing faults in electric vehicle charging equipment. Figure 5 and Table 3 show the diagnostic results of different models for faults. The traditional ELM model achieved the lowest fault diagnosis rate at 75.93%, while our proposed model reached the highest at 96.3%. This improved accuracy demonstrates the effectiveness of our algorithmic enhancements.

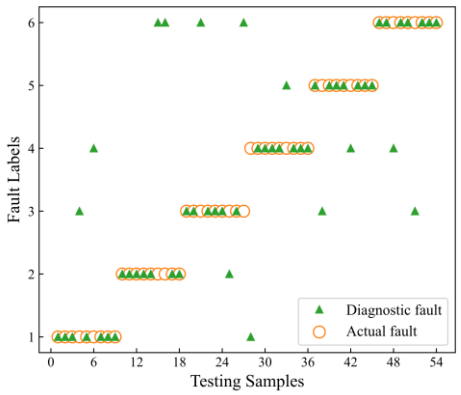


**(a)ELM diagnostic results**

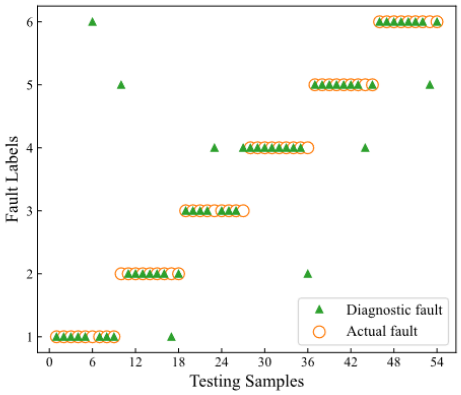


**(b)PSO-ELM diagnostic results**

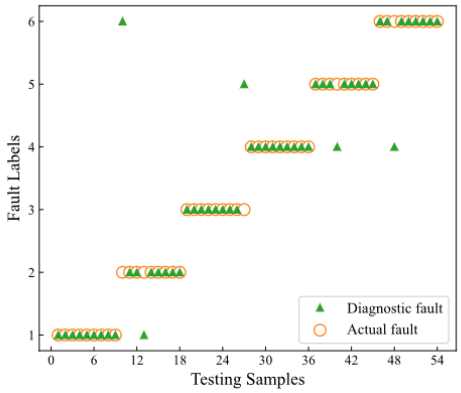


**(c)COA-ELM diagnostic results**

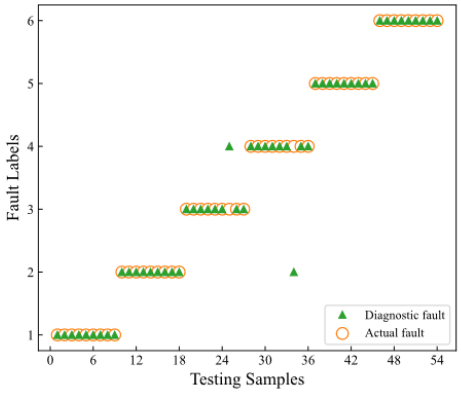


**(d)ACOA-ELM diagnostic results**

**Figure 5. Comparison of diagnostic results of different models**

**Table 3. Fault diagnosis results of the sample**

| Model | Average accuracy |
|---|---|
| ELM | 75.93% |
| PSO-ELM | 85.19% |
| COA-ELM | 90.74% |
| ACOA-ELM | 96.3% |

## V. DISCUSSION AND CONCLUSION

This article presents a novel fault diagnosis method for electric vehicle charging equipment utilizing an adaptive COA-ELM approach, aimed at enhancing the precision of fault detection. Through a comprehensive simulation analysis and subsequent discussions, the proposed model demonstrates strong predictive capabilities. When compared to other methodologies, it yields superior results, affirming the accuracy and effectiveness of the presented approach. The findings of this research can serve as valuable insights for the study and implementation of fault diagnosis in electric vehicle charging systems, offering the potential for more reliable and efficient solutions in practical applications related to fault diagnosis.

## VI. ACKNOWLEDGEMENT

Authors thanks the funding project, i.e., the technology project of State Grid Co. LTD. (Grant number: 5400-202440360A-3-1-KJ).

## REFERENCES

[1]. Gao H, Zang B B. New power system operational state estimation with cluster of electric vehicles[J]. Journal of the Franklin Institute, 2023, 360(12): 8918-8935.

[2]. Hou J J. Design and Implementation of State Monitoring and Remote Fault Diagnosis System for EV Charging Equipment [D]. Master of Thesis ,Qingdao, Qingdao University of Science and Technology, 2019

[3]. Gao H, Meng X, Qian K. Research on intelligent diagnosis strategy and treatment method of EV charging fault[C]//2019 5th International Conference on Control, Automation and Robotics (ICCAR). IEEE, 2019: 47-50.

[4]. Park S J, Kim W J, Kang B S. Development of a Fault-Diagnosis System through the Power Conversion Module of an Electric Vehicle Fast Charger[J]. Energies, 2022, 15(14): 5056.
[5]. Meckel S, Schuessler T, Jaisawal P K, et al. Generation of a diagnosis model for hybrid-electric vehicles using machine learning[J]. Microprocessors and Microsystems, 2020, 75: 103071.
[6]. Mao M, Dou Z, Chen L, Yang F, Liu H. Fault Diagnosis Method of Charging Pile Based on BOA-SSA-BP Neural Network. Journal of Jilin University Information Science Edition[J]. 2024,42(02):269-276.
[7]. Gao H, Liu Y F, Rong L N, Xie X P. Robust Consensus with Edge-based Multiplicative Uncertainties via Recursive Channel Filters[J]. IEEE Transactions on circuits and system II-Express Briefs, 2023, 70(7): 2550-2554.
[8]. Baik S H, ** Y G, Yoon Y T. Determining equipment capacity of electric vehicle charging station operator for profit maximization[J]. Energies, 2018, 11(9): 2301.
[9]. Zhang H. Impact of current ripple on electric vehicle charging equipment[C]//2016 International Conference on Civil, Transportation and Environment. Atlantis Press, 2016: 929-933.
[10]. Rigatti S J. Random forest[J]. Journal of Insurance Medicine, 2017, 47(1): 31-39.
[11]. Pal M, Parija S. Prediction of heart diseases using random forest[C]//Journal of Physics: Conference Series. IOP Publishing, 2021, 1817(1): 012009.
[12]. Kardani N, Bardhan A, Samui P, et al. A novel technique based on the improved firefly algorithm coupled with extreme learning machine (ELM-IFF) for predicting the thermal conductivity of soil[J]. Engineering with Computers, 2022: 1-20.
[13]. Shariati M, Armaghani D J, Khandelwal M, et al. Assessment of longstanding effects of fly ash and silica fume on the compressive strength of concrete using extreme learning machine and artificial neural network[J]. Journal of Advanced Engineering and Computation, 2021, 5(1): 50-74.
[14]. Jia H, Rao H, Wen C, et al. Crayfish optimization algorithm[J]. Artificial Intelligence Review, 2023, 56(Suppl 2): 1919-1979.
[15]. Fakhouri H N, Ishtaiwi A, Makhadmeh S N, et al. Novel hybrid crayfish optimization algorithm and self-adaptive differential evolution for solving complex optimization problems[J]. Symmetry, 2024, 16(7): 927.
[16]. Sorour S E, Hassan L, Abohany A A, et al. An improved binary crayfish optimization algorithm for handling feature selection task in supervised classification[J]. Mathematics, 2024, 12(15): 2364.
[17]. Maiti B, Biswas S, Ezugwu A E S, et al. Enhanced crayfish optimization algorithm with differential evolution's mutation and crossover strategies for global optimization and engineering applications[J]. Artificial Intelligence Review, 2025, 58(3): 69.
[18]. Li Z J, Li Y X, Lv X, et al. Research on moisture control at the inlet of leaf fil drying under different temperature and humidity conditions based on PSO-ELM. Acta Tabacaria Sinica,1-12[2025-01-15].